AGU PUBLICATIONS

Journal of Geophysical Research – Atmospheres

Supporting Information for

Southern Ocean low cloud and precipitation phase observed during the Macquarie Island Cloud and Radiation Experiment (MICRE)

Emily Tansey[1], Roger Marchand[1], Simon P. Alexander[2,3], Andrew R. Klekociuk[2,3], and Alain Protat[2,4]

[1]University of Washington, Seattle, Washington, United States

[2]Australian Antarctic Division, Hobart, TAS, Australia

[3]Australian Antarctic Partnership Program, Institute for Marine and Antarctic Studies, University of Tasmania, Hobart, TAS, Australia

[4]Australian Bureau of Meteorology, Melbourne, Victoria, Australia

Contents of this file

Text S1 to S2

Figures S1 to S3

Introduction

This document details in section S1 the calibration of the Australian Antarctic Division (AAD) lidar following O'Connor [2004], as well as a novel approach that scales the lidar backscatter to match that of the ceilometer in periods containing light below-cloud precipitation when the O'Connor method cannot be used. Section S2 describes an additional calibration of depolarization ratios from August-October, wherein we scale depolarization ratios from August-October by a constant factor calculated from liquid precipitation during the well-calibrated period prior.

S1. Polarization lidar backscatter calibration

We rely on both depolarization ratios and lidar backscatter measurements from the AAD polarization lidar (532 nm) obtained from April 6 to November 20 2016. Several sources of potential instability over the course of the time series were noted, namely three flashlamp changes (April 5, June 6 and Oct. 4) and an earthquake on Sept 8. In any case, we do not observe any notable increases in variability or performance degradation directly on or following these dates. Rather the lidar calibration is generally unstable throughout the 7 months (see Fig. S1). This instability is readily observable in the magnitude of the total (particulate + molecular) attenuated backscatter, and we therefore developed a time series of calibration scaling factors, as described below.

Initial calibration was based on measured photon counts in the height range 10 to 15 km, obtained during a clear-sky period on May 22, and matching the observed cross- and co-polar backscatter to that expected from molecular scattering. The near-surface aerosol optical depth was taken to be 0.05. The calibration is normalized with respect to laser output power and assumes an overlap correction. In spite of the overlap correction, there is an artifact (a narrow range with increased depolarization and total backscatter) near 250 m. This may or may not be indicative of some bias in the overlap correction, at least near the surface. Regardless, in this study we only used the data beyond 250 m to avoid this artifact.

We find that the total backscatter field in particular requires additional calibration. Starting with 5-minute backscatter, we apply the approach detailed in [O'Connor 2004]. This method requires cloud layers to be dense, liquid, optically thick, fully attenuating and non-precipitating, and thus nominally can only be applied to a small fraction of SO low clouds. O'Connor [2004] identified fully attenuated cloud layers as those that reduce the total backscatter by at least a factor of 20 from its in-cloud peak value within 300 m of the in-cloud peak. As noted in the main text of this paper, we loosen the criteria to include "heavily attenuating" clouds (backscatter drops by a factor of 10 within 600 m of the peak). Nonetheless, the total number of periods suitable to apply the calibration remains limited. The time series of calibration coefficients is shown in Fig. S1. Here the time series has been subject to additional noise filtering as shown in the flow chart in Fig. S2. Specifically, an O'Connor estimated calibration coefficient is initially determined on a 5-minute time scale (where the cloud is present for at least 1 minute). At the 5-minute scale, the cloud must be heavily or fully attenuating (as defined above). We do include precipitating clouds, and found that this made little difference in the overall calibrations. A 5-day running median (median of coefficients from that day and the surrounding ±2 days) is then taken.

Estimated values for the calibration coefficients that are more than factor of 2 from the 5-day median ($k_{5day}/2 < k$ or $k > 2\times k_{5day}$) are replaced by the median value. The resulting timeseries of calibration factors in shown by the blue line in Fig. S1.

In order to increase confidence in the calibration, we also calibrated the AAD lidar against the ARM ceilometer, whose calibration is stable (i.e. it appears to be constant in time when using the O'Connor technique). Specifically, we exploit the fact that for light (below-cloud) precipitation, one expects the total backscatter from the ceilometer and the AAD lidar to be the same. Here light precipitation means the contribution of multiple-scattering is small. We determine a transfer calibration coefficient (k_{tr}) by calculating the scale factor needed to make the AAD lidar backscatter match that measured by the ceilometer in below-cloud precipitation. The orange line in Fig. S1 shows the daily median of k_{tr}, including only periods where clouds are not fully or heavily attenuated where k_{tr} was used. The broad pattern is similar, with the calibration coefficient drifting upward until August, at which point there is a sizeable reduction with some recovery in late October. The similarity gives us some confidence that corrections are reasonable.

Rather than simply relying on either individual approach, the flowchart in Fig. S2 shows how the O'Connor and transfer calibrations are merged. When a fully or heavily attenuating cloud is present, the O'Connor estimate is used (left side of flowchart), and otherwise we compare the O'Connor calibration coefficient (which has been applied to a lightly attenuating cloud) to the k_{tr}. When $k'_{OConnor}$ (the prime denotes lightly attenuating) and k_{tr} match within a factor of 1/3, we simply use the average of the two as the estimated calibration factor. If they do not match, then we use average of the daily median of fully/heavily attenuating $k_{OConnor}$ coefficients (labeled k_{median} in the flowchart) and $k'_{OConnor}$. Ultimately, we found using averages (rather than k_{tr} alone or k_{median} alone) resulted in most accurately identifying the phase of cloud base correctly as liquid for warm clouds (CTT > 0°C). Nonetheless, a small fraction (5.8%) of the cases with light attenuation yields unphysical integrated attenuated backscatter ($\gamma < 0.02$ sr^{-1} or $\gamma > 0.2$ sr^{-1}). In these cases, we found defaulting to $k'_{OConnor}$ worked better than averaging with k_{tr} or k_{median}), such that only ~0.6% (1.1% in AM, 0.6% in JJA and 0.2% in SON) had unphysical values and were removed from the analysis (included in the "missing/bad data" fraction reported in Table #2 column 3).

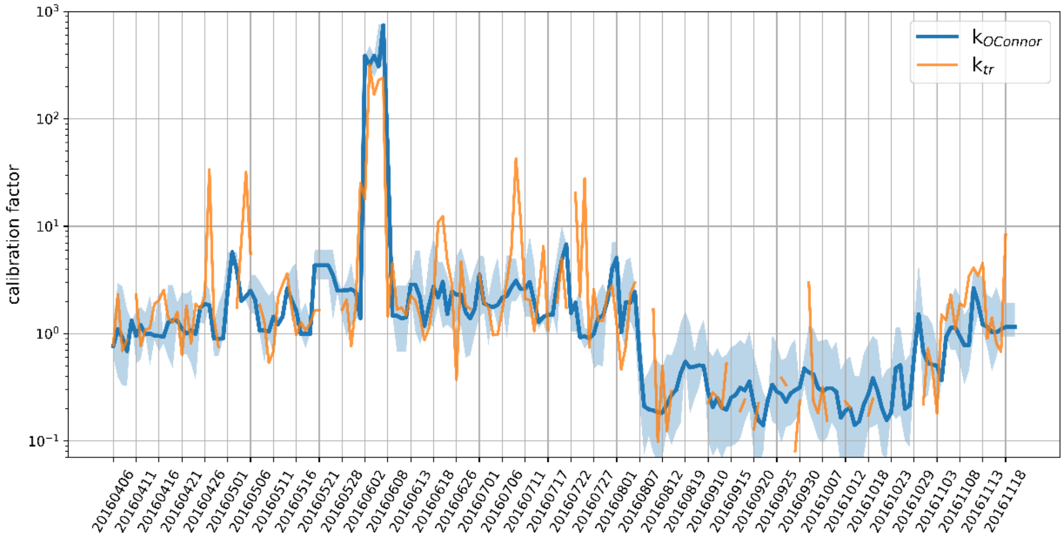

Figure S1: Time series of calibration coefficients calculated with the O'Connor method and subsequent filtering. The solid blue line represents the daily median, shading shows the daily range in calibration coefficients. The orange line is the daily median of transfer calibration coefficients; discontinuities in the orange line indicate where the transfer calibration was not applicable.

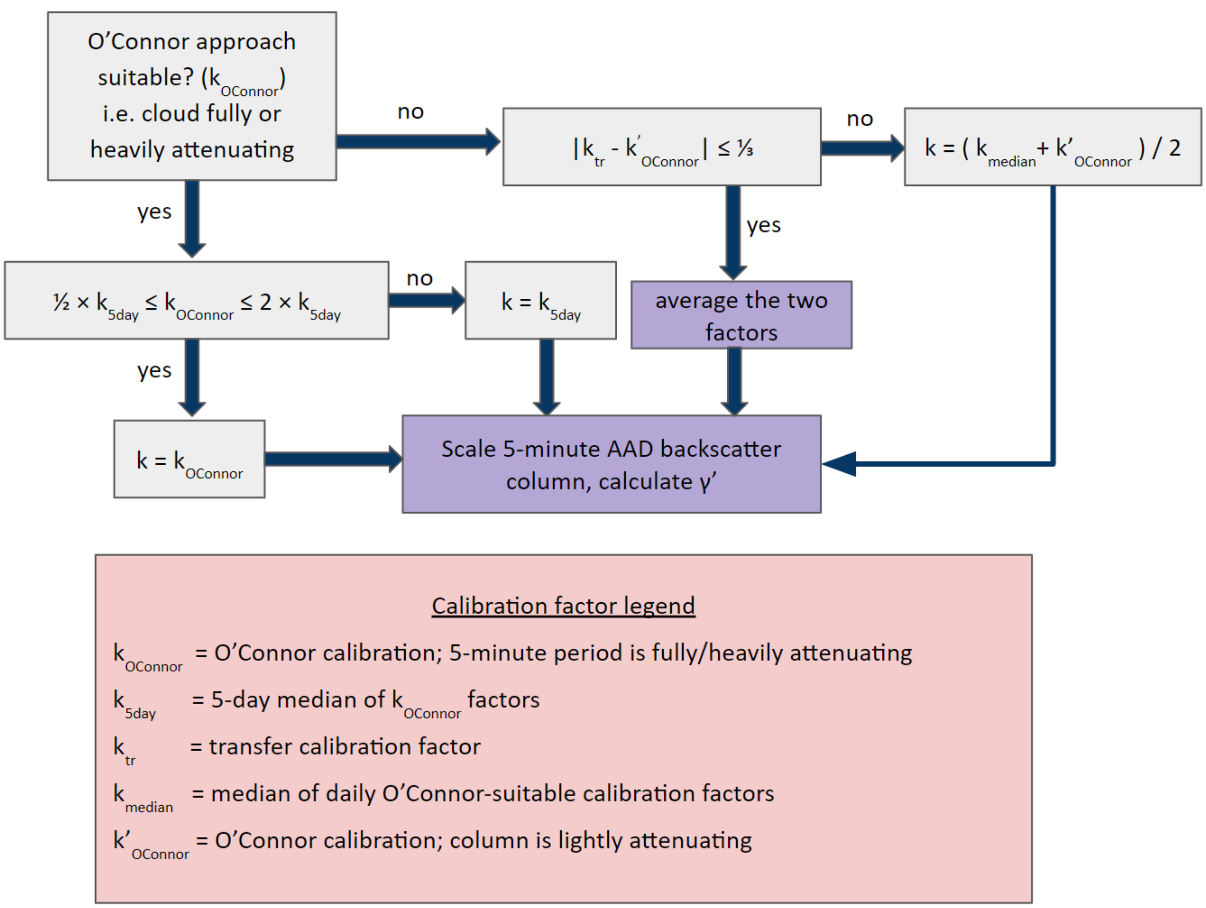

Figure S2: Flow chart of conditions to determine what calibration coefficient is used to scale the 5-minute lidar backscatter.

S2. Polarization lidar depolarization ratio calibration

The depolarization ratio, the ratio of the cross-to-co-polar backscatter (δ_L), also required a recalibration between August and October. As explained in Section S1, the original calibration was based on data collected in the May timeframe. The original AAD data contain an abrupt increase in the cross-polarization channel counts in August-October, resulting in a sizeable increase in δ_L (Fig. S3). The left panel of Fig. S3 shows a time series of δ_L for the below-cloud precipitation falling from warm-topped clouds in the original data. For light precipitation (where multiple scattering has little impact), we expect δ_L to be near-zero since spherical droplets should generate little to no cross-polarization. As the left panel shows, much of the time the below-cloud precipitation δ_L is near zero, until August and September (denoted by the red box). Note that Fig. S3 includes all below-cloud precip from warm clouds, not just light precipitation. Oddly, the depolarization ratio and (not shown) the cross-polarized backscatter return to pre-August levels near the beginning of November.

Taking the ratio of the mean cross-polarization counts before August during well-calibrated periods (6.8 counts) and during the period with elevated cross-pol from Aug.-Oct. (24 counts), we find a correction factor of 0.28. The resulting time series (right panel) after scaling by 0.28 during the bad period is shown in the right panel.

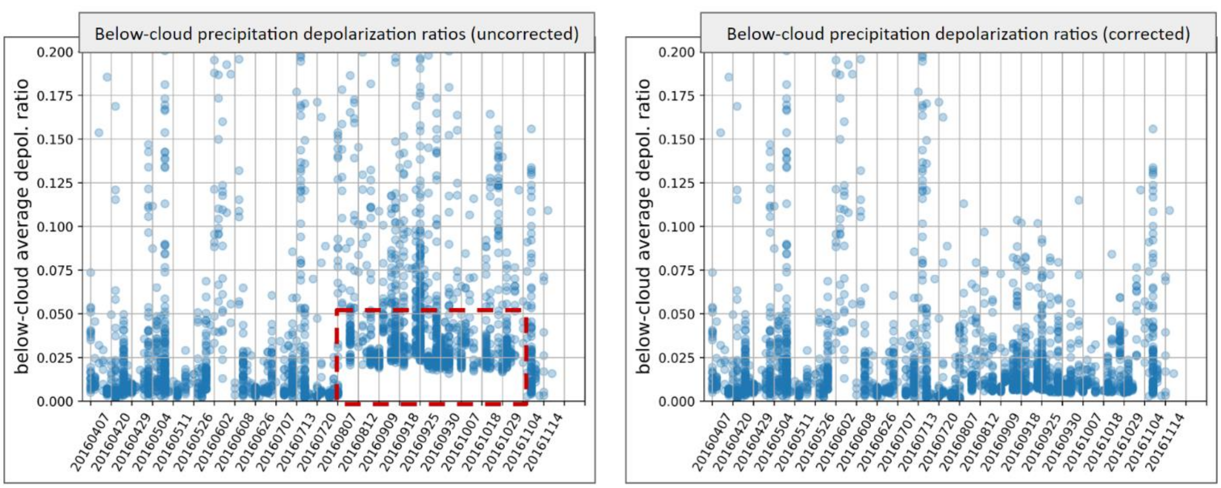

Figure S3: Time series of below-cloud depolarization ratios for warm-topped clouds before (left) and after (right) the calibration correction factor is applied. The red dashed box calls out the period where, due to an instrument malfunction, a step occurred in the cross-polarization channel counts, resulting in artificially raised depolarization ratios. The right plot is the depolarization time series after scaling the step by 0.28.